Investigation of Ion Separation by Microporous Nanofiltration Membranes

G. M. Rios and R. Joulie
Laboratoire des Matériaux et des Procédés Membranaires, Université de Montpellier II, 34095 Montpellier Cedex 05, France

S. J. Sarrade and M. Carlès
Commisariat à l'Energie Atomique (CEA), Rhône Valley Research Center, 26702 Pierrelatte Cedex, France

Two new nanofiltration membranes, an organomineral (titania-Nafion) medium and an inorganic (γAl_2O_3) medium, were studied using single or mixed solutions of monovalent or divalent ions. The experimental results not only confirm previous findings concerning the treatment of electrolytic solutions using charged nanofiltration membranes, but provide additional data notably for microporous membranes. A simple model based on the Nernst – Planck equation is proposed; its simplicity is related to the nature of the two membranes tested, for which the diffusion terms may easily be disregarded. It highlights the importance of the potential difference that forms on the membrane and explains most of the observed rejection results. In addition, ionic plugging of micropores may play a part with regards to rejection and flow depending on working conditions.

Introduction

In a previous study (Sarrade et al., 1994) the authors investigated the separation of uncharged polyethylene glycol solutes using two new nanofiltration membranes: an organomineral (titania-Nafion) medium and an inorganic (γAl_2O_3) medium. Dynamic characterization confirmed the results of static characterization and showed that both membranes behave as "microporous" media with a mean pore diameter slightly exceeding 1 nm, in which convection predominates over diffusion. A simple model of the transfer mechanisms was proposed, based on three parameters: the solvent permeability of the membrane, and the permeability and reflection coefficient characteristic of the selected solute.

This study was carried out with two membranes of the same type, but using single or mixed solutions of monovalent or divalent ions. Rejection performance was determined, and simple models are proposed that account at least qualitatively for the results, with emphasis on transfer mechanisms.

Experimental Investigation

Material and methods

Both membranes were fabricated and tested in the CEA's Membrane Laboratory at Pierrelatte by Sarrade et al. (1993). They are deposited on the inner face of a 155-mm-long tubular macroporous α alumina substrate (ID 7 mm, OD 10 mm).

One, designated the A membrane, is a strictly microporous inorganic layer, obtained by the sol-gel process. It is made from γ alumina, 2 μm thick and pore diameter around 1 nm.

The other (TN membrane) is obtained by depositing a thin film of Nafion, initially dissolved in an adequate solvant, onto a mesoporous titania membrane, laid itself on the α alumina substrate by the sol-gel process. The role of the titania intermediate layer (pore diameter: 10–20 nm; thickness: 1 μm) is just to correctly support Nafion. The polymer is fixed by gluing at the ends of the support. During manufacturing, the use of a removable organic layer between the inorganic underlayer and the thin top layer (about 0.1 μm) avoids the apparition of a superficial embedded layer (Sarrade et al., 1993).

The TN membrane was tested through various flow experiments reported elsewhere (Sarrade et al., 1996). Liquid water and supercritical carbon dioxide were used as solvent. From them it appears that J always varies linearly with ΔP, the transmembrane pressure. Moreover SC CO_2 to water permeability and water to SC CO_2 viscosity ratios are equal, which indicates that viscosity has a major influence as regards flux. Finally, the viscous flow model (Poiseuille) proves to be more

Correspondence concerning this article should be addressed to S. J. Sarrade.

convenient than the molecular flow equation (Knudsen) for the SC CO_2 flow description. All these data corroborate the idea that convection through micropores is the predominant transport mechanism.

From the viewpoint of nanoscopic heterostructure, these results may be related to data in the literature (Kelly et al., 1990; Dutta et al., 1990) indicating that Nafion is a tridimensional reticulate material, with internal cavities of about several nanometers in size and connective free-volume pathways. In what follows, the existence of micropores is assumed, even those with nonconventional characteristics.

Irrespective of the solution pH, the TN membrane is negatively charged; conversely, the charge of the A membrane is positive below, and negative above the material isoelectric point (pI) of about 8.3. This investigation was conducted with approximately neutral solution pH values (7) for which the A membrane was positively charged. The membranes were rinsed in osmosed water (Millipore Reverse Osmosis unit, water resistivity: 5 MΩ) between each test.

The test ions included Na^+, Mg^{2+}, Cl^-, and SO_4^{2-}. Experiments were conducted either with simple salt solutions (NaCl, Na_2SO_4, $MgCl_2$, or $MgSO_4$) or binary solutions ($NaCl/Na_2SO_4$ or $MgCl_2/MgSO_4$ for the TN membranes, and $NaCl/MgCl_2$ or $Na_2SO_4/MgSO_4$ for the A membranes). Four different concentrations (10^{-1} M, 10^{-2} M, 10^{-3} M, and 10^{-4} M) were tested for the simple solutions; Table 1 indicates their reduced ionic strength, together with an estimate of the mean hydrated radius given by Rosset (1984) and the free diffusivity in water reported by Newman (1991). For the binary solutions, the counterion concentration (cations for TN membranes, anions for A membranes) was maintained constant at 10^{-3} M, and the molar fractions of the two coions varied in the following ratios: 0/1, 0.2/0.8, 0.5/0.5, 0.8/0.2, and 1/0; the ionic strength, which depends on the molar ratios, remained within the limits of the single-salt solutions (i.e., 0/1 and 1/0). For example Table 1 indicates the ionic strength of various $NaCl/Na_2SO_4$ mixtures. The cation concentrations in the permeate and rejection residue were determined by atomic absorption, while ion chromatography was used for the anions.

The membranes were tested in a conventional pilot facility that has already been described by Sarrade et al. (1994). The permeate and retentate streams were continuously recycled, allowing steady-state concentrations to be reached in less than an hour. The working temperature θ was 303 K, the tangential flow velocity U was 2 $m \cdot s^{-1}$, and the membrane pressure gradient ΔP was 1, 2 or 3 MPa, for simple salt solutions. For binary mixtures all the runs were conducted at 1 MPa.

Table 1. Ionic Strength, Hydrated Radius, and Water Diffusivity

Salt	I/C_s	Ion	r (10^{-10} m)	D (10^{-9} $m^2 s^{-1}$)
NaCl	1	Na^+	4	1.3
Na_2SO_4	3	Mg^{2+}	8	0.7
$MgCl_2$	3	Cl^-	3	2.0
$MgSO_4$	4	SO_4^{2-}	4	1.0

For an NaCl (C_s)/Na_2SO_4 (αC_s) mixture with a constant cation concentration $C_{s_+} = (1+2\alpha)C_s$:

$$I/C_{s_+} = 0.5\left[1 + \frac{1+4\alpha}{1+2\alpha}\right]$$

that is, 1 if $\alpha = 0$; 1.17 if $\alpha = 0.25$; 1.33 if $\alpha = 1$; 1.44 if $\alpha = 4$; 1.5 if $\alpha = \infty$.

By definition: $I = 0.5 \sum z_i^2 \cdot C_i$

Table 2. TN Membrane

Salt	Pres. MPa	10^{-4} M J	10^{-4} M R	10^{-3} M J	10^{-3} M R	10^{-2} M J	10^{-2} M R	10^{-1} M J	10^{-1} M R
NaCl	1	34.4	22.0	37.4	12.0	35.4	10.0	36.4	4.0
	2	66.7	28.0	64.7	15.0	65.4	10.0	74.8	5.0
	3	97.0	34.0	101.1	20.0	115.2	19.0	111.2	11.0
Na_2SO_4	1	38.4	65.0	46.5	71.0	38.4	68.0	31.3	39.0
	2	76.8	76.0	78.8	76.0	75.8	74.0	63.7	52.0
	3	109.2	79.0	115.2	80.0	99.0	78.0	101.1	56.0
$MgCl_2$	1	46.5	47.0	50.5	32.0	45.5	32.0	44.5	30.0
	2	80.9	57.0	83.0	41.0	91.0	49.0	85.0	36.0
	3	123.3	64.0	121.3	43.0	145.6	55.0	131.4	40.0
$MgSO_4$	1	40.4	60.0	46.5	52.0	47.5	58.0	32.3	59.0
	2	91.0	69.0	89.0	60.0	80.9	61.0	63.7	63.0
	3	135.5	71.0	111.2	63.0	141.5	65.0	105.1	67.0

J: $L \cdot h^{-1} \cdot m^{-2}$; R: %

Results and discussion

The fluxes (J) and the apparent rejection factors ($R = 1 - C_p/C_o$) obtained for the simple solutions are indicated in Tables 2 and 3. Higher J values were observed for the TN membrane; the flux varied in a virtually linear manner with ΔP regardless of the experimental system tested (Figures 1, 3 and 4). While the slope of the curves varied only slightly with the solution concentration, it depended to a greater extent on the nature of the salt. This linear evolution is generally consistent with a primarily convective solvent transfer mechanism and a low-concentration polarization due to the type of solution used. The latter assertion is clearly supported by the estimated actual rejection factors ($R^* = 1 - C_p/C_m$) for the two lowest concentrations (Table 4). A conventional calculation procedure was used, based on the film theory:

$$J = k \cdot \ln\left(\frac{C_m - C_p}{C_o - C_p}\right)$$

Table 3. A Membrane

Salt	Pres. MPa	10^{-4} M J	10^{-4} M R	10^{-3} M J	10^{-3} M R	10^{-2} M J	10^{-2} M R	10^{-1} M J	10^{-1} M R
NaCl	1	12.2	43.0	15.5	50.0	19.2	47.0	14.1	11.0
	2	24.0	67.0	34.4	63.0	32.3	58.0	44.5	15.0
	3	34.4	89.0	49.5	67.0	50.6	61.0	60.7	24.0
Na_2SO_4	1	14.1	34.0	20.2	25.0	18.2	24.0	12.1	16.0
	2	30.7	51.0	35.4	32.0	39.4	26.0	30.3	17.0
	3	58.6	62.0	58.6	41.0	62.7	31.0	40.4	26.0
$MgCl_2$	1	24.3	89.0	29.3	96.0	25.2	96.0	25.2	67.0
	2	44.5	95.0	52.6	97.0	45.0	96.0	40.4	75.0
	3	60.7	97.0	80.9	97.0	70.0	96.0	62.7	76.0
$MgSO_4$	1	30.3	31.0	25.2	30.0	25.3	9.0	22.2	8.0
	2	60.6	48.0	43.5	36.0	50.5	11.0	40.4	9.0
	3	91.0	60.0	72.8	38.0	80.9	10.0	64.7	11.0

J: $L \cdot h^{-1} \cdot m^{-2}$; R: %

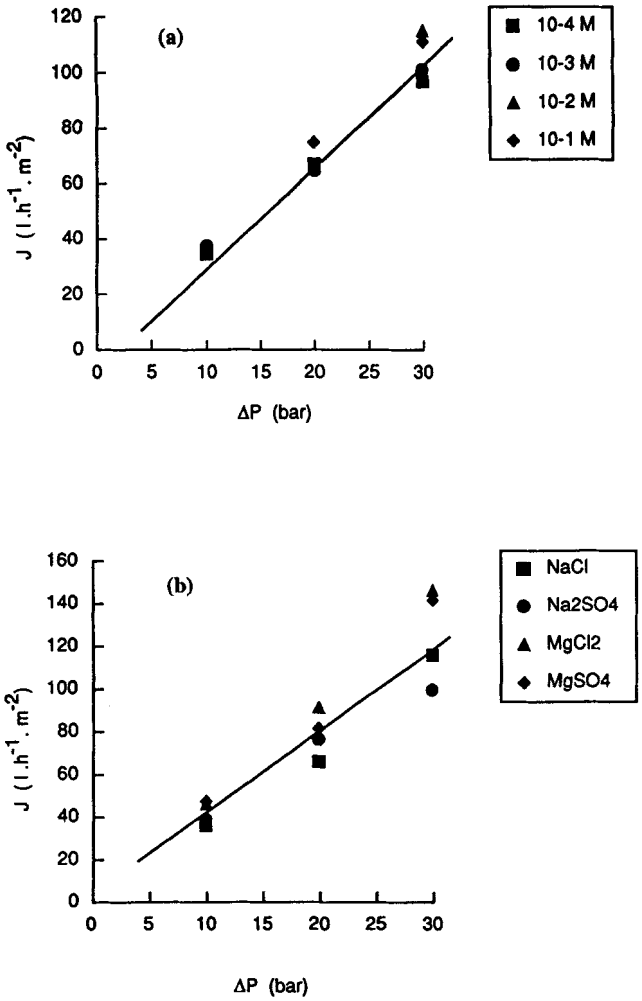

Figure 1. TN membrane: J vs. ΔP.

(a) NaCl solutions at various concentrations; (b) various solutions at 10^{-2} M.

and Deissler's equation:

$$Sh = 0.023\ Re^{0.875} \cdot Sc^{0.25},$$

where kinetic viscosity $\upsilon = 8 \times 10^{-7}$ m^2·s^{-1} and diffusion coefficient $D = 1.3 \times 10^{-9}$ m^2·s^{-1} on average (Table 1), hence, $Re = 17{,}500$, $Sc = 640$, $Sh = 600$, and the mass-transport coefficient $k = 1.1 \times 10^{-4}$ m·s^{-1}.

The operating conditions did not allow exhaustive analysis of the results, but the rejection trends observed with simple solutions corresponded to ion exclusion by electric effect (notably the Donnan effect). This is consistent with the findings reported by other authors, generally using negatively charged organic membranes Nielsen and Jonsson (1994) or Tsuru et al. (1991a,b) or, less frequently, with an oppositely charged ceramic, as in Alami-Younssi et al. (1994). Figures 2–4 illustrate the following points:

- Although the electrolytes were of small dimensions, all were significantly rejected.
- For any given salt, the nature of the material had a major effect on rejection.
- The rejection increased with the valence of the coion.
- The rejection diminished as the concentration increased.
- The rejection diminished as the counterion valence increased.

The rejection values were very high for $MgCl_2$ with membrane A, and near 100% between 10^{-4} M and 10^{-2} M. This result may be ascribed to the conjunction of five favorable factors: suitable valences for the coion (2+) and counterion (1−), a porous medium with low permeability (i.e., low J), a large cation (Table 1), and probably a strong electric charge on the material itself.

With binary solutions, J varied appreciably depending on the proportions of the two coions—especially with the TN membrane, for which the permeation flow rate virtually doubles when the two anions are present in equal amounts compared with the limit (single-ion) solutions (Table 5). This is an original observation that has not been widely reported in the literature. Moreover, the TN membrane did not reject the monovalent anion: negative rejection was even observed, as already noted in the literature by Tsuru et al. (1991a,b). The monovalent anion thus passes through the filter element with the cation. Similar remarks may be made concerning the A membrane (Table 6), although the J and R variations were of lower amplitude, and negative rejection was not observed. Care was taken during these binary solution tests to maintain a fixed counterion concentration; under these conditions the drop in the coion rejection was observed more clearly as the counterion valence increased. Figure 5 shows that the calculated counterion rejection (for the $NaCl/Na_2SO_4$ solution in

Table 4. Estimated Actual Rejection Factors

Salt	Pres. MPa	10^{-4} M (TN)		10^{-3} M (TN)		10^{-4} M (A)		10^{-3} M (A)	
		R, %	R^*, %	R, %	R^*, %	R, %	R^*, %	R, %	R^*, %
NaCl	1	22.0	24.0	12.0	13.0	43.0	44.0	50.0	52.0
	2	28.0	32.0	15.0	18.0	67.0	71.0	63.0	65.0
	3	34.0	41.0	20.0	25.0	89.0	90.0	67.0	70.0
Na_2SO_4	1	65.0	68.0	71.0	74.0	34.0	35.0	25.0	27.0
	2	76.0	80.0	76.0	80.0	51.0	52.0	32.0	34.0
	3	79.0	84.0	80.0	85.0	62.0	66.0	41.0	58.0
$MgCl_2$	1	47.0	50.0	32.0	33.0	89.0	90.0	96.0	96.0
	2	57.0	62.0	41.0	44.0	95.0	96.0	97.0	97.0
	3	64.0	70.0	43.0	49.0	97.0	98.0	97.0	97.0
$MgSO_4$	1	60.0	63.0	52.0	56.0	31.0	35.0	30.0	32.0
	2	69.0	75.0	60.0	67.0	48.0	55.0	36.0	40.0
	3	71.0	79.0	63.0	71.0	60.0	70.0	38.0	46.0

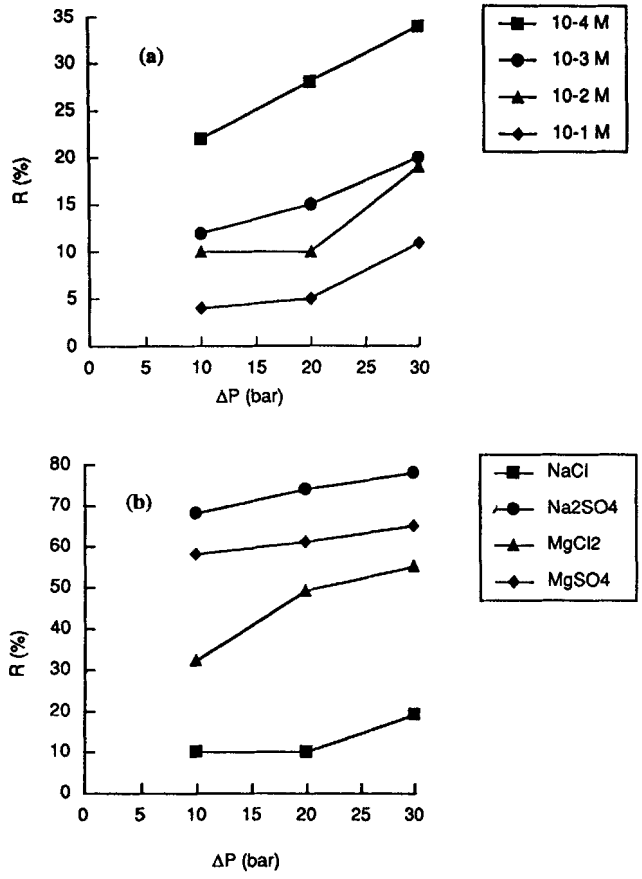

Figure 2. TN membrane: rejection percentage vs. ΔP.

(a) NaCl solutions at various concentrations; (b) various solutions at 10^{-2} M.

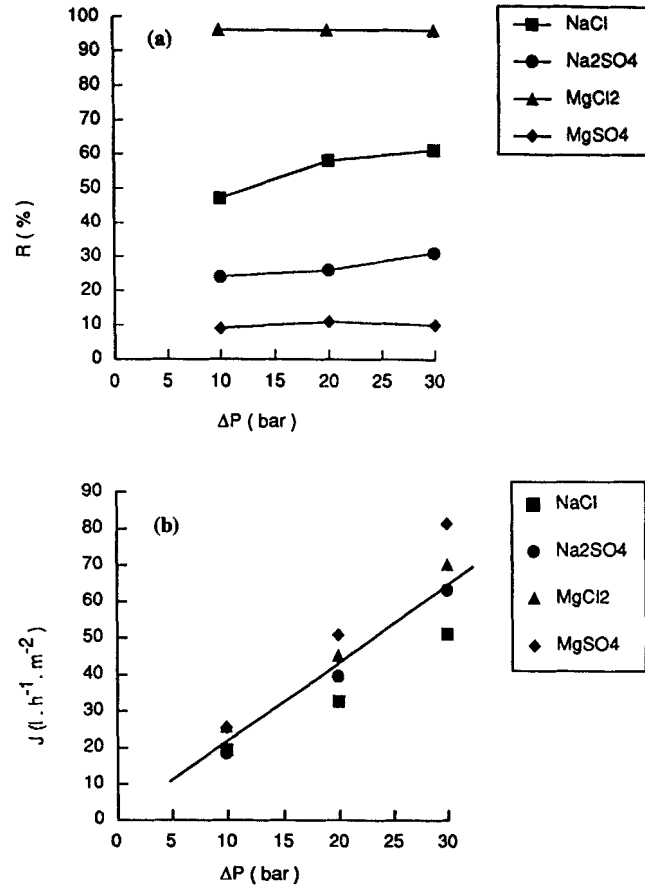

Figure 3. A membrane: various solutions at 10^{-2} M.

(a) Rejection percentage vs. ΔP; (b) J vs. ΔP.

this case) decreased regularly as the proportion of the monovalent coion increased.

Theoretical Interpretation

General principles

Reference is frequently made to the Nernst–Planck equation (e.g., Mulder (1991) and Tsuru et al. (1991a,b)) in modeling water and ion transfer in a nanofiltration membrane. This equation integrates all the driving forces, and may be established by a Stefan-Maxwell approach presented by Wesselingh and Krishna (1990). For low concentrations (10^{-4} M or even 10^{-3} M), the activities and concentrations may be considered equivalent as the salt activity coefficients are near 1. The equation may then be written in differential form:

$$J_i = -U_i\left[\frac{dC_i}{dX} + \frac{C_i Z_i F}{RT}\cdot\frac{d\phi}{dX}\right] + JC_i(1-\sigma_i), \qquad (1)$$

where

J_i = molar flux of i ($\text{mol}\cdot\text{m}^{-2}\cdot\text{s}^{-1}$)
J = solvent flux ($\text{m}\cdot\text{s}^{-1}$)
U_i = diffusivity or mobility of i ($\text{m}^2\cdot\text{s}^{-1}$)
C_i = concentration of i ($\text{mol}\cdot\text{m}^{-3}$)
Z_i = valence of i
F = Faraday constant ($\text{C}\cdot\text{mol}^{-1}$)
R = ideal gas constant ($\text{J}\cdot\text{mol}^{-1}\cdot\text{K}^{-1}$)

Table 5. TN Membrane

Salts	Cl^- Fraction	SO_4^{2-} Fraction	J	R (Cl^-)	R (SO_4^{2-})
$NaCl/Na_2SO_4$	0%	100%	39.1	—	68.0
	20%	80%	70.7	2.0	56.0
	50%	50%	72.7	−7.0	58.0
	80%	20%	68.7	−4.0	60.0
	100%	0%	37.4	12.0	—
$MgCl_2/MgSO_4$	0%	100%	46.5	—	52.0
	20%	80%	70.7	−28.0	39.0
	50%	50%	86.0	−8.0	41.0
	80%	20%	74.8	7.0	44.0
	100%	0%	47.3	32.0	—

Table 6. A Membrane

Salts	Na^+ Fraction	Mg^{2+} Fraction	J	R (Na^+)	R (Mg^{2+})
$NaCl/MgCl_2$	0%	100%	26.0	—	93.0
	20%	80%	29.3	48.0	96.0
	50%	50%	30.3	44.0	95.0
	80%	20%	30.3	50.0	97.0
	100%	0%	15.5	50.0	—
$Na_2SO_4/MgSO_4$	0%	100%	25.2	—	30.0
	20%	80%	30.3	0.0	29.0
	50%	50%	38.0	0.0	32.0
	80%	20%	35.4	10.0	38.0
	100%	0%	20.2	25.0	—

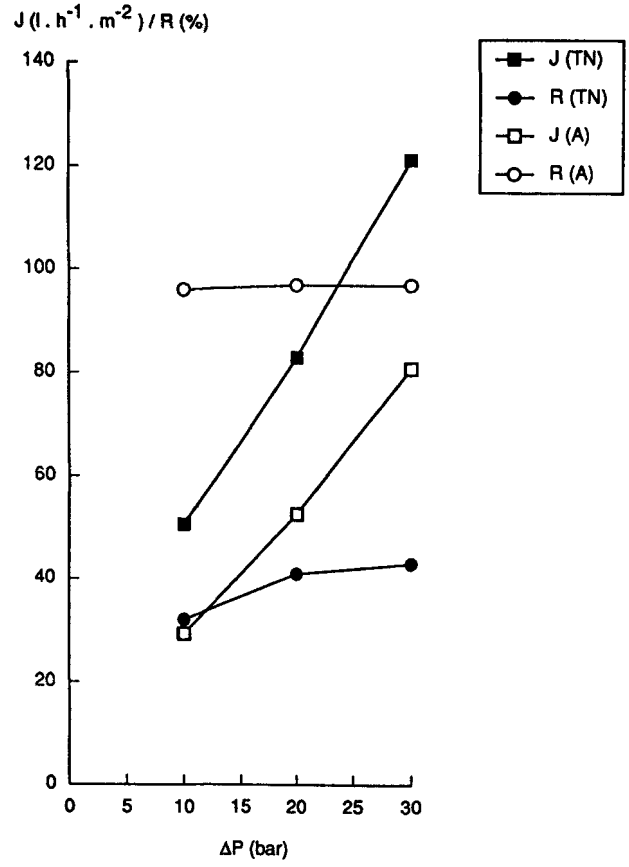

Figure 4. $MgCl_2$ (concentration = 10^{-3} M).

T = temperature (K)
ϕ = electrostatic potential (V)
σ_i = reflection coefficient of i
X = distance variable (m)

For the membranes investigated here, the diffusion part in mass transfer is several times lower than the convection, as previously described by Sarrade et al. (1994); the equation may thus be simplified as follows:

$$J_i = -U_i \cdot \frac{C_i Z_i F}{RT} \cdot \frac{d\phi}{dX} + JC_i(1-\sigma_i). \qquad (2)$$

The existence and the sign of the electrostatic potential difference, hereafter referred to as *flow potential*, may be explained considering the electrokinetic phenomena in the pores. These phenomena are of particular importance in nanofiltration because of the small channel dimensions. Figure 6 indicates schematically how the potentials are distributed normally and in the immediate vicinity of a charged surface (inherent charge or adsorbed ions) in the absence of electrical neutrality (cf. Perry's handbook (1984)). Fluid flow along the wall will create a flow potential that may be related to the fluid tangential velocity ν by a law of the following type:

$$\nu = -\epsilon \cdot \frac{d\phi}{dX} \cdot \frac{\zeta}{\mu}, \qquad (3)$$

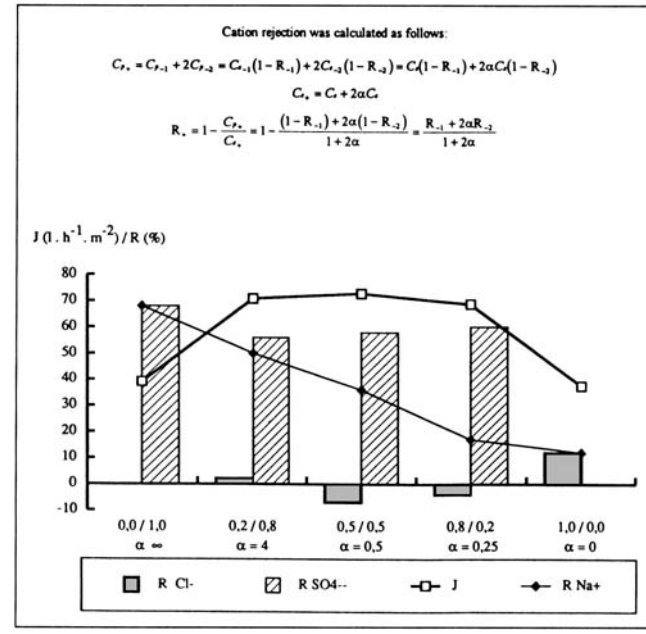

Figure 5. TN membrane; Na^+ cation.

where ϵ is the solution permittivity, μ its viscosity, and ζ the potential difference in the diffuse mobile layer ("zeta potential") that depends on the solution and interface properties. Depending on whether ζ is positive or negative (membrane charge), the flow potential will be negative or positive, respectively.

The following discussion first considers a simple salt solution with monovalent cation and anion (e.g., NaCl) with a negatively charged TN membrane; other salts and the posi-

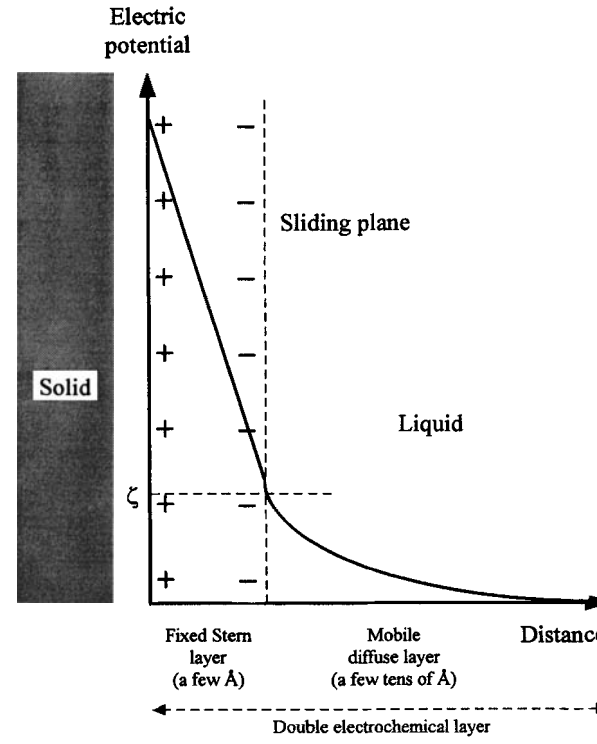

Figure 6. Electrokinetic phenomena.

tively charged A membrane are then considered, before extending the scope to mixtures of ionic species.

Monovalent cation and anion salt (NaCl) and negatively charged membrane (TN)

Integrating Eq. 2 over the entire thickness e of the membrane allows the cation and anion permeate flow densities to be written in the following form:

$$JC_{p_+} = -P_+ \bar{C}_+ \Delta\Psi + J\bar{C}_+(1-\sigma_+) \tag{4}$$

$$JC_{p_-} = +P_- \bar{C}_- \Delta\Psi + J\bar{C}_-(1-\sigma_-), \tag{5}$$

where $\Delta\Psi = F\Delta\phi/RT$ (reduced flow potential), $P_+ = U_+/e$ and $P_- = U_-/e$ (membrane cation and anion permeability), and $\bar{C}_+$ and $\bar{C}_-$ are the mean cation and anion concentrations.

Considering that electrically neutral conditions prevail in the permeate, it follows that:

$$\bar{C}_+[J(1-\sigma_+) - P_+\Delta\Psi] = \bar{C}_-[J(1-\sigma_-) + P_-\Delta\Psi]. \tag{6}$$

If a Donnan equilibrium is assumed to exist between the solution and membrane at the pore inlets, as postulated by Tsuru et al. (1991a,b), then it is expressed by allowing for $\bar{C}_M$ (the mean membrane charge concentration):

$$C_{s_+}C_{s_-} = \bar{C}_+\bar{C}_- \cong \bar{C}_M\bar{C}_-, \tag{7}$$

where $\bar{C}_- = (C_s^2/\bar{C}_M)$, and C_{s_+}, C_{s_-}, and C_s are the cation, anion, and total salt concentrations in solution. Hence;

$$\bar{C}_M[J(1-\sigma_+) - P_+\Delta\Psi] = \frac{C_s^2}{\bar{C}_M}[J(1-\sigma_-) + P_-\Delta\Psi] \tag{8}$$

or

$$\Delta\Psi = J\cdot\frac{(1-\sigma_+) - K(1-\sigma_-)}{P_+ + KP_-}, \tag{9}$$

where $K = (C_s^2/\bar{C}_M^2)$. This expression indeed confirms the existence of a positive flow potential $\Delta\Psi$ for low C_s, and thus K values, since reflection coefficients are less than 1.

Figure 7 is a diagram of the system concentrations and potentials, and $\Delta\Psi_S$ and $\Delta\Psi_P$ represent the established potential differences at interfaces. The figure shows that $\Delta\Psi_S$ hinders anion migration while favoring cation flow; $\Delta\Psi$ and $\Delta\Psi_P$ have the opposite effect. These are the phenomena controlling rejection.

If σ_i and P_i represent the mechanical and electrical frictions that control, respectively, the convection and migration contributions to the movement of ion i according to the Stefan-Maxwell approach, then consistent with Eq. 9 it is logical to assume that, for a given coion, the counterion displacement properties have a dominant role:

$$J\uparrow \Rightarrow \Delta\Psi\uparrow \quad \text{if} \quad \sigma_+\downarrow \quad \text{or if} \quad P_+\downarrow, \tag{10}$$

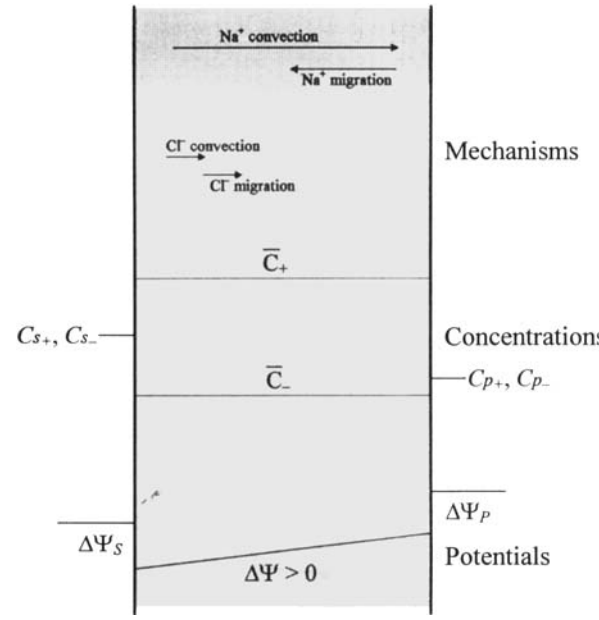

Figure 7. Ion transport diagram.

and that the coion effect is enhanced as the concentration rises in solution (as K increases) with:

$$J\uparrow \Rightarrow \Delta\Psi\uparrow \quad \text{if} \quad \sigma_-\uparrow \quad \text{or if} \quad P_-\downarrow \tag{11}$$

The fact that the rejection diminishes as the concentration in solution rises at a constant ΔP may be qualitatively explained by a drop in the upstream Donnan potential—because the mean anion concentration in the membrane increases according to Eq. 7—and in $(\Delta\Psi/J)$—thus the cation back motion diminishes according to Eq. 4. The following relation, based on Eq. 5 and Eq. 7, also shows that (C_{p_-}/C_{s_-}) increases and the rejection diminishes:

$$\frac{C_{p_-}}{C_s} = \frac{C_{p_-}}{C_{s_-}} = +P_-\cdot\frac{C_s}{\bar{C}_M}\cdot\frac{\Delta\Psi}{J} + \frac{C_s}{\bar{C}_M}\cdot(1-\sigma_-). \tag{12}$$

Conversely, on the basis of the preceding comprehensive equations, it appears more difficult to account for the fact that the rejection rises systematically, if only moderately, when ΔP is increased at constant C_s (Tables 2 and 3). The explanation may involve other elements not taken into account in the model, such as fouling phenomena at pore entrance. Considering the similar dimensions of ions and micropores, this assumption is realistic. Increasing ΔP would favor water movement, thus diluting the permeate.

Extension to other simple solutions and/or membranes

The preceding discussion may be extended to other types of salts and membranes. Table 7 lists the expressions describing the Donnan equilibrium for the four salts and the two oppositely charged membranes studied here. Table 8 indicates the equations for determining $\Delta\Psi$ in each case, and the extended cation and anion flow equations are shown below:

$$JC_{p_+} = -P_+ z_+ \bar{C}_+ \Delta\Psi + J\bar{C}_+(1-\sigma_+) \tag{13}$$

Table 7.

	Negative Charge	Positive Charge
$C_s = C(\text{NaCl})$	$\bar{C}_- = \frac{C_s^2}{C_M}$	$\bar{C}_+ = \frac{C_s^2}{C_M}$
$C_s = C(\text{Na}_2\text{SO}_4)$	$\bar{C}_- = \frac{4C_s^3}{C_M^2}$	$\bar{C}_+ = \sqrt{\frac{8C_s^3}{C_M}}$
$C_s = C(\text{MgCl}_2)$	$\bar{C}_- = \sqrt{\frac{8C_s^3}{C_M}}$	$\bar{C}_+ = \frac{4C_s^3}{C_M^2}$
$C_s = C(\text{MgSO}_4)$	$\bar{C}_- = \frac{2C_s^2}{C_M}$	$\bar{C}_+ = \frac{2C_s^2}{C_M}$

$$JC_{p_-} = + P_- z_- \bar{C}_- \Delta\Psi + J\bar{C}_-(1-\sigma_-). \qquad (14)$$

Several conclusions may be drawn from these elements:

- If the membrane is positively charged, then $\Delta\Psi < 0$ as already noted.
- The absolute value of $\Delta\Psi$ increases if the coion valence increases or if the counterion valence diminishes according to the expressions in Table 8, that is, the rejection increases for the same mobile charge concentration (Eqs. 13 and 14). Transfer mechanisms in the membrane thus produce effects similar to those of the simple Donnan equilibrium (Table 7).
- Similar remarks may be made concerning the effects of the solution concentration or the working pressure.
- The rejection variations are enhanced by more highly charged membranes (as appears to be the case with the ceramic membrane A).

All these findings are in agreement with those of Tsuru et al. (1991a,b).

Salt mixtures

Consider a mixture of NaCl (C_s) and Na_2SO_4 (αC_s) with a negatively charged membrane. Proceeding as before, we get:

$$JC_{p_+} = - P_+ \bar{C}_+ \Delta\Psi + J\bar{C}_+(1-\sigma_+) \qquad (15)$$

$$JC_{p_{-1}} = + P_{-1}\bar{C}_{-1}\Delta\Psi + J\bar{C}_{-1}(1-\sigma_{-1}) \qquad (16)$$

$$JC_{p_{-2}} = + P_{-2}2\bar{C}_{-2}\Delta\Psi + J\bar{C}_{-2}(1-\sigma_{-2}), \qquad (17)$$

where the -1 and -2 subscripts refer to mono- and divalent anions.

Electrical neutrality of the permeate (i.e., $C_{p_+} - C_{p_{-1}} - 2C_{p_{-2}} = 0$) implies that

$$\bar{C}_+[J(1-\sigma_+) - P_+\Delta\Psi] = \bar{C}_{-1}[J(1-\sigma_{-1}) + P_{-1}\Delta\Psi] + 2\bar{C}_{-2}[J(1-\sigma_{-2}) + 2P_{-2}\Delta\Psi]. \qquad (18)$$

Assuming once again that the mean cation concentration is near $\bar{C}_M$, the Donnan equilibrium conditions for each pair (cation/anion$_1$ and cation/anion$_2$) are then:

$$C_{s_+}C_{s_{-1}} = \bar{C}_+\bar{C}_{-1} \cong \bar{C}_M\bar{C}_{-1} = (1+2\alpha)C_s^2 \qquad (19)$$

$$C_{s_+}^2 C_{s_{-2}} = \bar{C}_+^2\bar{C}_{-2} \cong \bar{C}_M^2\bar{C}_{-2} = \alpha(1+2\alpha)^2 C_s^3, \qquad (20)$$

hence

$$[J(1-\sigma_+) - P_+\Delta\Psi] = K_1[J(1-\sigma_{-1}) + P_{-1}\Delta\Psi] + K_2[J(1-\sigma_{-2}) + 2P_{-2}\Delta\Psi] \qquad (21)$$

where

$$K_1 = \frac{(1+2\alpha)C_s^2}{C_M^2} \quad \text{and} \quad K_2 = \frac{2\alpha(1+2\alpha)^2 C_s^3}{C_M^3},$$

that is,

$$\Delta\Psi = J\cdot\frac{(1-\sigma_-) - K_1(1-\sigma_{-1}) - K_2(1-\sigma_{-2})}{P_+ + K_1P_{-1} + 2K_2P_{-2}}. \qquad (22)$$

In this study, the cation concentration $(1+2\alpha)C_s$ is constant at 10^{-3} M. If this value is designated K, then

$$K_1 = \frac{K^2}{(1+2\alpha)C_M^2} \quad \text{and} \quad K_2 = \frac{2\alpha K^3}{(1+2\alpha)C_M^3}. \qquad (23)$$

As α increases (i.e., if the molar fraction of the divalent anion increases), then K_1 diminishes and K_2 rises. For moder-

Table 8.

Salt	Negative Charge $\Delta\Psi = J\cdot\frac{(1-\sigma_+) - K(1-\sigma_-)}{z_+P_+ - Kz_-P_-}$	Positive Charge $-\Delta\Psi = J\cdot\frac{(1-\sigma_-) - K(1-\sigma_+)}{z_-P_- - Kz_+P_+}$
NaCl	$K = \frac{C_s^2}{C_M^2} = K^*$	
Na_2SO_4	$K = 8\frac{C_s^3}{C_M^3} = K^*\left(8\frac{C_s}{C_M}\right)$	$K = \sqrt{8\frac{C_s^3}{C_M^3}} = K^*\sqrt{\left(8\frac{C_M}{C_s}\right)}$
$MgCl_2$	$K = \sqrt{8\frac{C_s^3}{C_M^3}} = K^*\sqrt{\left(8\frac{C_M}{C_s}\right)}$	$K = \frac{8C_s^3}{C_M^3} = K^*\left(8\frac{C_s}{C_M}\right)$
$MgSO_4$	$K = \frac{4C_s^2}{C_M^2} = 4K^*$	

ate α values, however, both the value and variation rate of K_1 will exceed those of K_2: at low C_s values, the K/C_M ratio is well below 1. Moreover, the $1/(1+2\alpha)$ and $2\alpha/(1+2\alpha)$ functions both have derivatives with the same absolute value. Assuming that σ_{-1} and σ_{-2} are close, then $\Delta\Psi/J$ may be considered to increase with α. By equating $\overline{C}_M$ and $\overline{C}_+$, Eq. 15 shows that C_{p_+} diminishes as α increases, and accounts for the observed increase in cation rejection. Since $C_{s_{-1}} = C_s$, Eq. 16 and Eq. 19 may be combined as follows:

$$\frac{C_{p_{-1}}}{C_s} = \frac{C_{p_{-2}}}{C_{s_{-1}}} = \frac{K}{\overline{C}_M}\left(P_{-1}\frac{\Delta\Psi}{J} + (1-\sigma_{-1})\right) = 1 - R_{-1}. \quad (24)$$

This equation confirms that the monovalent anion rejection decreases as α increases.

Similarly, combining Eq. 17 and Eq. 20:

$$\frac{C_{p_{-2}}}{\alpha C_s} = \frac{C_{p_{-2}}}{C_{s_{-2}}} = \frac{K^2}{\overline{C}_M^2}\left(P_{-2}\frac{\Delta\Psi}{J} + (1-\sigma_{-2})\right) = 1 - R_{-2} \quad (25)$$

shows that the divalent anion rejection also decreases. In any event, the absolute value of R_{-2} will always be well above R_{-1} because of the multiplier factor K/C_M, and it will vary at a lower rate (despite the factor of 2 weighting the divalent ion migration term). All these phenomena may be observed in Figure 5 for the lowest α values.

Similar interpretations may be advanced for other mixtures, and correctly account for the observed behavior of the A and TN membranes (Tables 5 and 6).

It is difficult to account for the optimum flux recorded with intermediate α values on the basis of conventional solvent permeability notions. Figure 5 suggests that it may be related to the drop in rejection, notably for the monovalent coion; similar remarks may also be made for the other systems investigated. One can think of a reduction in the fixed Stern-layer thickness in the presence of both coions. Under these conditions, the increased permeate flow rate would be attributable to a decrease in peripheral pore plugging.

Conclusions

The experimental results obtained in this investigation generally confirm published findings concerning the treatment of simple or mixed electrolytic solutions using charged nanofiltration membranes. These results provide additional data, notably with regard to microporous membranes (most authors have used dense membranes derived from reverse-osmosis applications, while in this case the material may be considered as an optimized ultrafiltration medium)—especially when positively charged (very few studies have covered this subject to date, and only with simple solutions).

A model based on the Nernst–Planck equation is proposed; its simplicity is related to the nature of the two membranes tested, for which the diffusion terms may easily be disregarded. The model highlights the importance of the potential difference that forms on the membrane, and which explains most of the observed rejection results. This electrokinetic parameter depends on the nature of the process solution and on the membrane geometry and electric charge. This is reflected in the equations by allowance for the permeate flow and for the ion reflection and permeability coefficients. Unlike the Donnan effect, which tends to reject the coions on the system input side, that is, in the feed solution, this flow potential facilitates their passage through the pores.

Another significant aspect of this work is the suggestion that, contrary to dense membranes, with fine microporous membranes variations in ionic fouling due to charges in operating conditions may induce variations in flow and rejection. This working hypothesis accounts for results that would be difficult to interpret on the basis of conventional solvent permeability considerations: for example, permeate flow-rate variations observed in mixtures when only the proportion of the salts differ; or R increasing with ΔP in simple solutions; or the dependence of the slope of the $J(\Delta P)$ curves on the selected ionic solute.

Additional data must be compiled before fully implementing the model for predictive purposes, notably the permeability/reflection coefficients for each ion, their degree of hydration, and the actual charge of the membrane material.

Literature Cited

Alami-Younssi, S., A. Larbot, M. Persin, J. Sarrazin, and L. Cot, "Gamma Alumina Nanofiltration Membrane: Application to the Rejection of Metallic Cations," *J. Memb. Sci.*, **91**, 87 (1994).

Dutta, B. K., D. Randolph, and S. K. Sikdar, "Thin and Composite High-flux Membranes of Perfluorosulfonated Ion-exchange Polymer," *J. Memb. Sci.*, **54**, 51 (1990).

Kelly, J., H. M. Meunier, D. E. McCormack, A. Michas, and M. Pineri, "Uranyl Ions in Perfluorinated (Nafion and Flemion) Membranes: Spectroscopic and Photophysical Properties and Reactions with Potassium Hydroxide," *Polymer*, **31**, 387 (1990).

Mulder, M., *Basic Principles of Membrane Technology*, Chap. 5, Kluwer, London (1991).

Newman, J. S., *Electrochemical Systems*, 2nd ed., Prentice Hall, Englewood Cliffs, NJ (1991).

Nielsen, D. W., and G. Jonsson, "Bulk-Phase Criteria for Negative Ion Rejection in Nanofiltration of Multicomponent Salt Solutions," *Sep. Sci. Technol*, **29**(9), 1165 (1994).

Perry's Chemical Engineer Handbook, 6th ed., McGraw-Hill, New York, pp. 17–34, 36 (1984).

Rosset, R., "Equilibres Chimiques en Solutions," *Tech. Ing.*, J1800, Paris (1984).

Sarrade, S., C. Bardot, M. Carlès, R. Soria, S. Cominotti, and R. Gillot, "Elaboration of New Multilayer Membranes for Nanofiltration," *Proc. World Filtration Congress*, Nagoya, Japan, p. 955 (1993).

Sarrade, S., G. M. Rios, and M. Carlès, "Dynamic Characterization and Transport Mechanisms of Two Inorganic Membranes for Nanofiltration," *J. Memb. Sci.*, **97**, 155 (1994).

Sarrade, S., G. M. Rios, and M. Carlès, "Nanofiltration Membrane Behavior in a Supercritical Medium," *J. Memb. Sci.*, in press (1996).

Tsuru, T., M. Urairi, S. I. Nakao, and S. Kimura, "Negative Rejection of Anions in the Loose Reverse Osmosis Separation of Mono- and Divalent Ion Mixtures," *Desalination*, **81**, 219 (1991a).

Tsuru, T., S. I. Nakao, and S. Kimura, "Calculation of Ion Rejection by Extended Nernst-Planck Equation with Charged Reverse Osmosis Membranes for Simple and Mixed Electrolyte Solutions," *J. Chem. Eng. Japan*, **24**(4), 511 (1991b).

Wesselingh, J. A., and R. Krishna, *Mass Transfer*, Ellis Horword Ser. in Chem. Eng., London (1990).

Manuscript received Aug. 11, 1995, and revision received Jan. 19, 1996.